ELSEVIER

Microelectronics Reliability 44 (2004) 993–1007

MICROELECTRONICS RELIABILITY

www.elsevier.com/locate/microrel

Pull-off test in the assessment of adhesion at printed wiring board metallisation/epoxy interface

Markus P.K. Turunen [a,*], Pekka Marjamäki [a], Matti Paajanen [b], Jouko Lahtinen [b], Jorma K. Kivilahti [a]

[a] *Department of Electrical and Communications Engineering, Laboratory of Electronics Production Technology, Helsinki University of Technology, P.O. Box 3000, FIN-02015 HUT, Sahkotalo 1, Finland*

[b] *Department of Engineering Physics and Mathematics, Laboratory of Physics, Helsinki University of Technology, P.O. Box 1100, FIN-02015 HUT, Sahkotalo, Finland*

Received 5 September 2003; received in revised form 23 December 2003
Available online 4 February 2004

Abstract

It is shown that the value of adhesion strength at the metallisation/polymer interface can be determined directly from a printed wiring board (PWB) by a pull-off method. However, careful optimisation of the test geometry is required. In particular, the mechanical properties of the substrate are important. The use of flexible substrate in the test results in severe underestimation of the adhesion strength. There was a considerable stress peak at the edge of the test area, as shown by a finite element method (FEM) calculation with the flexible construction. This unevenly distributed stress decreases the force needed to detach the coating. In addition, if the test area is not defined to match the stud of the test equipment, the stress peak appears at the adhesive/coating interface rather than at the coating/metallisation interface. The experimental data and the examination of the fracture surfaces by scanning electron microscope (SEM) were consistent with the FEM results. In addition, the effect of environmental stresses on the adhesion was investigated. The environmental tests consisted of exposures to (1) thermal shock, (2) elevated temperature and relative humidity and (3) corrosive gases NO_2, SO_2, H_2S and Cl_2. The employment of embedded capacitors during the exposures revealed the diffusion of water into the epoxy, which weakened the adhesion. The corrosive gases induced irreversible deterioration of the dielectric material. An adhesion promoter enhanced the durability of the coating/Cu interface in the environmental tests. X-ray photoelectron spectroscopy was used to analyse the chemical states of the pre-treated copper surfaces.

1. Introduction

It is essential that the quality of interfacial adhesion is controlled in the manufacture of electronic devices. Of equally great concern is the durability of the adhesion in the changing—and often harsh—environments that consumer products are exposed to. Environmental factors accelerate degradation processes until eventually failure mechanisms like corrosion, fatigue, fracture and wear take over. Materials with physically and chemically different properties are frequently combined in electronics and the adhesion between dissimilar materials is particularly susceptible to these failure mechanisms. A fundamental understanding of the compatibility between different materials is essential as the miniaturisation of electronics continues [1–6].

Since the expected lifetime of an electronic device is measured in years, accelerated tests have to be employed

Abbreviations: PWB, printed wiring board; FEM, finite element method; SEM, scanning electron microscope or scanning electron microscopy; PDE, photodefinable epoxy; FMG, flowing mixed gas; GPS, 3-glysidoxy propyl trimethoxy silane; UV, ultraviolet; RH, relative humidity; EDS, energy dispersive spectroscopy; XPS, X-ray photoelectron spectroscopy

* Corresponding author. Tel.: +358-9-451-2716; fax: +358-9-451-5776.

E-mail address: markus.turunen@hut.fi (M.P.K. Turunen).

0026-2714/$ - see front matter © 2004 Elsevier Ltd. All rights reserved.
doi:10.1016/j.microrel.2004.01.001

to assess the interfacial reliability within reasonable time scales. Several accelerated tests are used to induce failure modes resembling those occurring in normal use [1,7]. The thermo-mechanical compatibility of interfaces in electronic devices is studied by subjecting them to thermal cycling. The sequential exposure to low and high temperatures causes dimensional changes within a polymer coating and a substrate, but of different magnitudes because of a mismatch in the coefficients of thermal expansion. The interfacial adhesion prevents the adaptation of coating to the changed stress state and stresses are induced in the plane of the coating [8]. These stresses can be relaxed by molecular motion within polymer coatings. However, the molecular motion, and thus the stress relaxation are restricted in the thermosetting epoxy coating because of the dense covalent crosslinks. Finally, if the accumulated stress exceeds the tolerance of the coating/substrate system—unavoidably—it relaxes by the formation of cracks in the coating [9] or by interfacial delamination [10].

The effects of moisture on reliability are studied by placing the specimens in a chamber where the relative humidity and temperature can be adjusted to levels that accelerate the diffusion of water into polymeric structures and, at the same time, increase the rate of corrosion of metals [1]. Moisture can affect the adhesion of polymeric materials in many ways. Absorbed water causes a volume expansion inducing stresses within the polymer layer [11], but it also acts as a plasticiser [12], which reduces the deteriorating effect of the induced dimensional changes because the molecular motion becomes easier. However, the plasticisation also decreases the glass transition temperature and weakens the mechanical properties of the polymer [13–15]. Depending on the polymer chemistry, moisture can cause irreversible changes in the bulk polymer by causing further crosslinking, chemical or physical degradation [11,16, 17]. Water can also attack the adhesive bonds across the polymer/substrate interface [11,15,18–20]. Added to the loss of adhesion, high humidity compromises the electrical performance of electronic components and dielectrics [1,21,22]. Eventually, if a sufficient electric field exists, the corrosion products start to migrate between the electrodes (i.e. electrochemical migration) and, in the worst case, short the electrical circuits [23].

The telecom and automotive industries are concerned with environmental effects at the level of both complete assembly and individual components. Malfunction of electrical contacts and connectors is particularly likely to occur in environments rich in corrosive gases. To take into account the effect of gaseous air pollutants on reliability, the selected gases are employed at elevated relative humidity and temperature. This flowing mixed gas (FMG) test usually includes the use of nitrogen dioxide (NO_2), sulphur dioxide (SO_2), hydrogen sulphide (H_2S) and chlorine (Cl_2) in different concentrations depending on the simulated environment (coastal, heavy industrial, tropical, rural, indoor, etc.) [24–26]. Much work has been carried out to characterise the electrochemical reactions that take place on metal surfaces during FMG exposures [24,25,27–30]. Surprisingly, however, electronic devices have rarely been tested under FMG conditions, even though the effects of these typical atmospheric contaminants on the reliability are indisputable [31]. To our knowledge, the effects of FMG exposure on the adhesion between copper and epoxy have not yet been investigated. It should to be noted, however, that the use of accelerated tests in reliability assessment is not always straightforward since the harsh environments used to achieve the acceleration effect may seriously affect the failure mechanisms [29].

In earlier work we have studied the adhesion of deposited copper to several photodefinable epoxy (PDE) [32–34] and other polymer substrates [35,36]. However, the results cannot be applied to the adhesion of polymer coating to copper substrate; for if copper is deposited on a smooth epoxy surface, no measurable adhesion is achieved [32], whereas good adhesion is achieved if the epoxy is applied on a smooth copper surface [3,37]. Thus, the deposition sequence is of importance to the obtainable adhesion. It follows that different factors must be taken into consideration in the design of the adhesion test depending on the uppermost material (copper or epoxy) that is to be detached from its substrate. Comprehensive reviews are available on the various adhesion test geometries as well as of the mechanics and mechanisms of adhesion failure [4,5,38–40].

In the present work we applied a pull-off test to study the adhesion of a photodefinable epoxy coating to the copper surface of a standard PWB substrate. Advantages and pitfalls of the test are discussed. Since the reliability of build-up modules [2] is affected by moisture, ionic contaminants, temperature fluctuations, etc. [6,11, 12,23,41,42], we also applied selected environmental tests, to evaluate the influence of environmental factors on the adhesion.

2. Experimental

2.1. Materials

A copper metallised glass fibre reinforced epoxy (FR-4) printed wiring board was used as the base substrate. The preparation of the photodefinable epoxy (PDE) solution from Epikote-157 (Shell) resin has been presented elsewhere [43]. γ-Butyrolactone (Aldrich) was used as solvent in the development of the test pads. Thermally curable epoxy adhesive was used to attach the stud of the adhesion test equipment to the coatings. The materials for the electroless deposition procedure of the copper plate capacitors have been described earlier

[33]. Photo mask (Riston MM140 from DuPont) was utilised in the subtractive fabrication of the interdigital capacitors on the PWB using a copper etching solution (Ultraincide 35/35 from Alfachimici). 3-Glysidoxy propyl trimethoxy silane (GPS) was obtained from Dow Corning and applied to the copper as an adhesion promoter. A pure (99.95 at.%) reference copper sheet (0.5 mm) was used for chemical analysis of the treated copper surfaces and for monitoring the performance of the FMG equipment.

2.2. Procedure for preparation of the test structures

Before use, the copper surfaces were cleaned according to Appendix A in the IEC 68-2-60 standard. The procedure included cathodic degrease in 1 N NaOH (for 15–30 s at 5–10 V), using a platinum anode, and dipping in H_2SO_4 (10 wt% in water) for 20–30 s. After each treatment step the specimens were rinsed with deionised water and dried. The oxidation pre-treatment of the copper surfaces was carried out in an aqueous solution (pH = 9) with use of a platinum cathode. The potential difference (5.0 V) was controlled with an EG&G Princeton Applied Research Potentiostat/Galvanostat (Model 263A). The adhesion promoter (GPS) was applied on surfaces from a 1 wt% solution in water by dipping the samples in the water solution and baking at 120 °C for 30 min.

The PDE solution was spin-coated on the pre-treated printed wiring board substrates (12 cm × 12 cm) at a speed of 1100 rpm for 60 s. The coatings were approximately 30–40 μm in thickness. After the spin-coating, the samples were pre-baked at 90 °C for 30 min to remove the solvent, and exposed to ultraviolet (UV) light (365 nm, 17 mW/cm^2) for 40 s. Two-step crosslinking was started with a 30 min bake at 120 °C and followed by 60 min at 140 °C in a convection oven. Development of adhesion test pads was carried out between the crosslinking bakes. A schematic presentation of the process flow of the adhesion test specimen preparation is given in Fig. 1. This approach enables simultaneous preparation of multiple adhesion test pads. The adhesion tests were also carried out from nonphotodefined coatings. Both flexible and rigid constructions were evaluated. In the rigid construction the PWB was attached with the adhesive to a 1-cm thick iron sheet, whereas the flexible construction tests were carried out directly from the PWB. Sufficient adhesion at the adhesive/coating interface was achieved without special pre-treatments by a simple washing of the coating surface with isopropanol and deionised water prior to the stud attachment. It is assumed that there are a sufficient number of unreacted epoxy groups on the coating surface able to form covalent bonds with the adhesive and provide the necessary adhesion at the particular interface.

Plate capacitors were fabricated on a PWB and the lower electrodes were prepared using a subtractive technique. The upper electrodes were plated fully additively on the PDE coating [2]. Both open and embedded capacitors were prepared. The area of the plate capacitor was 25 mm^2.

The interdigital capacitors were prepared on the PWB by the subtractive technique. The spacing between the conductors was 125 μm. Both open and PDE coated capacitors were prepared. The interdigital capacitors were operated under 9.0 V bias at the 85 °C/85% RH and FMG conditions.

2.3. Pre-treatment of aluminium studs

For execution of a pull-off test, the stud of the test equipment has to be firmly attached to the coating. To ensure this, thorough surface treatment of the stud was carried out. Hydrocarbon-based surface contaminants were removed by solvent degreasing in acetone, after which the stud was immersed for 12 min (at 70 °C) in an etching solution prepared from deionised water (100 g), H_2SO_4 (30 g) and $Na_2Cr_2O_7$ (6 g). Finally, the studs were washed in running deionised water and dried at 60 °C for 30 min.

Fig. 2 shows a SEM micrograph of the pre-treated aluminium stud. The micrograph shows that a porous surface has formed. The adhesive can fill in the pores and, upon thermal crosslinking, it becomes mechanically interlocked into the stud surface. The inherently weak adhesion between the aluminium stud and adhesive is thus improved. We note, however, that excess etching results in too porous surface, which then acts as a weak boundary layer during the adhesion test. Sandblasting and rubbing with sandpaper were also tested as methods of surface pre-treatment, but both merely increased the roughness without providing porosity.

2.4. Environmental tests

Three test procedures were used to expose the test specimens to environmentally induced stresses. All the tests were carried out at the Laboratory of Electronics Production Technology, Helsinki University of Technology. The first test combined elevated temperature and relative humidity (RH) and was conducted in the Weiss SB 1180 apparatus according to the IEC 68-2-67 standard at 85 ± 2 °C and 85 ± 5% RH for 1000 h. The test was also applied at 25 ± 2 °C and 75 ± 5% RH. The second test was FMG exposure, which was carried out in the Weiss WK1 600 environmental chamber equipped with facilities for controlled dosage of corrosive gases. This test combines the effects of relative humidity (75 ± 5% RH), temperature (25 ± 2 °C) and corrosive gases. The IEC 68-2-60 standard (method 4) was applied for 1000 h and the following

corrosive gases were applied: NO_2 (200 ± 20 ppb), SO_2 (200 ± 20 ppb), H_2S (10 ± 5 ppb) and Cl_2 (10 ± 5 ppb). The performance of the test chamber was monitored with copper sheets and an analysis of the gas concentrations. In a deviation from the standard, the concentration of chlorine gas was based on the calculated design value not actually measured. A third test, thermal shock, was carried out in the Weiss TS 130 apparatus for 1000 h (2000 cycles) according to the IEC 68-2-14N standard ($+125 \pm 2$ °C/-45 ± 2 °C, dwell 15 min/15 min). Embedded and open capacitors were placed in the environmental chambers simultaneously with the adhesion test specimens. The capacitance of the plate capacitors was monitored.

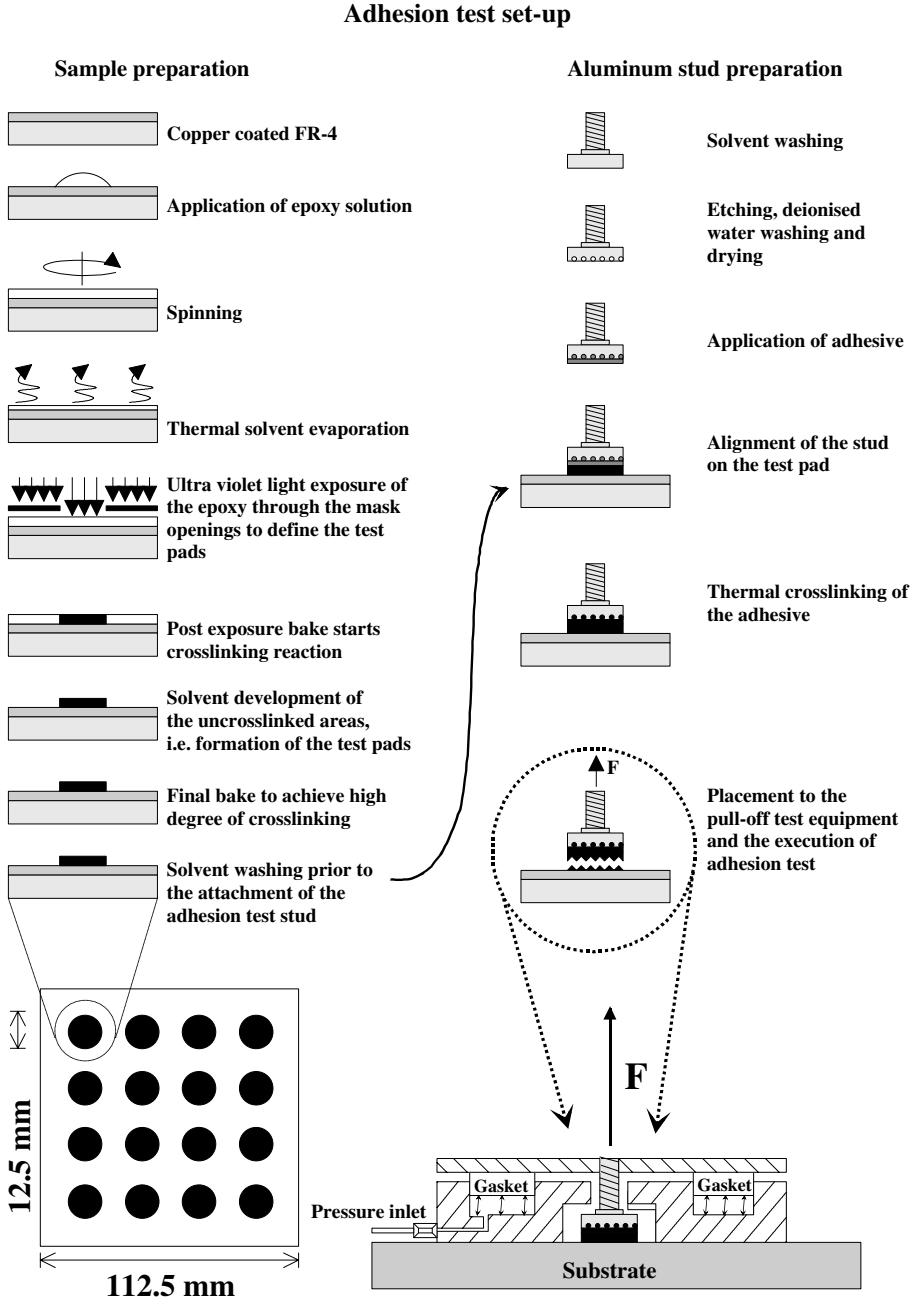

Fig. 1. Schematic presentation of the preparation of the adhesion test pad and the execution of the adhesion test with the pull-off equipment.

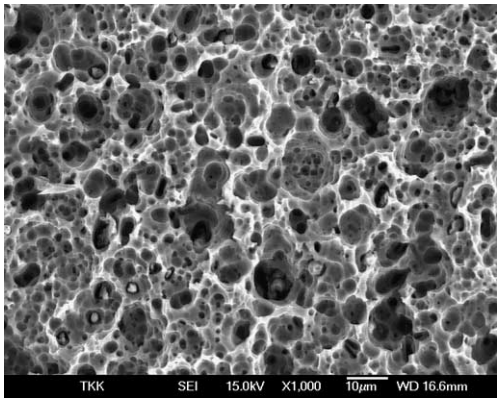

Fig. 2. Scanning electron micrograph of the pre-treated aluminium stud showing the microporous surface that enables mechanical interlocking of the adhesive.

2.5. Characterisation

The topography of the treated aluminium stud surface (tilted at 45°), as well as the fracture surfaces of the adhesion specimens (polymer side only), were examined with a field emission scanning electron microscope (SEM). Before the examination the specimens were sputter-deposited with chromium. Energy dispersive spectroscopy (EDS) elemental mapping was used to detect electrochemical migration of corrosion products.

The adhesion testing for the copper/PDE systems was carried out with an Elcometer 110 P.A.T.T.I.® pneumatic tester according to the ASTM D4541-95e1 standard. The diameter of the stud was 12.5 mm. The stud was attached to the PDE surface with a thermally curable epoxy adhesive (baking at 140 °C for 30 min). The results are the averages of 16 repeated tests done on each system.

The X-ray photoelectron spectra of the untreated and treated copper surfaces were recorded with an SSX-100 X-ray photoelectron spectroscope (XPS). A monochromatic Al Kα X-ray source was used. Measurements were made at a pressure of 10^{-7} Pa. Peak fitting was done with fully Gaussian peaks and Shirley background subtraction. The measured X-ray photoelectron spectrum is not exactly the same as the emission spectrum of the sample because the emitted electrons can undergo inelastic scattering within the sample, which results in electron energy losses. The original emission spectrum can be re-gained by subtracting the background. The background is mostly formed of the noise of the detection electronics and the inelastically scattered electrons.

Shirley [44] has presented a method, now widely used, for the background subtraction. This method assumes that all emitted electrons have the fixed probability of scattering, regardless of their original kinetic energy and the energy loss involved. The background count rate at any energy is thus proportional to the integral of the count rates of electrons with higher energies. This leads to an iterative method. Although the Shirley background subtraction assumes fixed probabilities of scattering due to different kinetic energy, it is widely used because it is reproducible and because no parameters are involved. Other background subtraction methods include simple linear subtraction (which has no supportive physical theory) and the Tougaard background subtraction (which needs parameters). After the background subtraction, the peaks are fitted to the spectra assuming that the individual emission "lines" form a Gaussian distribution. Gaussian distribution is a result of the detection electronics, and due to the original energy levels of the electrons, which are a distribution rather than discrete values. All elemental concentration calculations were based on the high-resolution spectra.

A Hewlett-Packard PM 6632B Automatic RCL-Meter was used in the electrical characterisation of the capacitors at 1 MHz frequency.

2.5.1. Finite element modelling

Modelling of the test was carried out with the finite element program ABAQUS. The model consisted of a part of the stud and a part of the substrate. The stud was cut 12 mm above the substrate and the substrate was cut 14.5 mm from the axis of symmetry. The adhesive layer was set to be 10 μm, the PDE 35 μm and the copper layer 18 μm in thickness. The model was made up of two-dimensional axisymmetric linear continuum elements, except for the copper layers, on both surfaces of the substrate where membrane elements were used. The model consisted of two parts, which were tied together using the TIE option in ABAQUS. One part was of the stud edge area where the element size was 2.5 μm, while the other part was of the rest of the stud and the PWB where the element size was 0.2 mm.

Pulling force was applied as a concentrated load to the top edge of the stud. The force was 368 N, which results in 3 MPa tensile stress providing that the stress is distributed uniformly. Upward movement of the substrate was prevented on the part of the top surface of the substrate lying 12.5–14.5 mm from the axis of symmetry. When the effect of a rigid substrate was studied, also the upward displacement of the whole lower surface of the substrate was prevented.

All materials were considered as elastic. Polymers usually behave in a viscoelastic manner but the effect of this was considered to be negligible as the aim was to study the relative effect of different set-ups, not to obtain actual stress values. The material properties used in the calculations are shown in Table 1. The properties of FR4 are orthogonal, but here only one value was used for all directions.

Table 1
Mechanical parameters of the materials used in the study

	Stud (aluminium)	FR-4 substrate (epoxy composite)	Adhesive (epoxy)	PDE (epoxy)	Substrate metal (copper)
E (GPa)	71	18.6	3.2	8	120
υ	0.3	0.25	0.4	0.22	0.3

3. Results and discussion

3.1. Adhesion testing

The adhesion strength between the photodefinable epoxy (PDE) and the copper metallisation of a printed wiring board (PWB) was measured by the pull-off method. Fig. 1 shows the attachment of the stud to the coating. There are two problems that have to be dealt with in order to carry out a reliable test. First, the adhesive adheres poorly to the aluminium stud of the test apparatus if proper pre-treatment is not performed. Secondly, although it is common to execute the test by attaching the stud at an arbitrary place on the coating surface, this may lead to an erroneous interpretation of the test results. Accordingly, the adhesion tests were carried out from both a photodefined, i.e. partially PDE-coated copper and from a PDE whole coating. Later on in the text, the term "nonphotodefined" refers to test set-ups where the adhesion tests were run at an arbitrary point on the coating. The term "photodefined", in turn, refers to tests that were carried out from precisely photodefined test pads of the epoxy coating, which were exactly the same in area as the stud of adhesion test equipment. The results of the photodefined and nonphotodefined test set-ups are compared, and factors affecting the reliable execution of the pull-off test are discussed.

3.1.1. Verification of the method—modelling

The main drawback in running an adhesion test from a sample that is build-up on a flexible substrate is that the stresses are highly concentrated at the edges of the stud. Bending of the substrate during the test causes uneven distribution of the stress. Fig. 3 shows the tensile stress distributions as calculated by the finite element method (FEM) for flexible and rigid substrates. Comparison of the flexible and rigid substrates reveals a clear difference in the area where the stress is concentrated. In the case of the flexible substrate, the highest stress at the copper/PDE interface is about 30 times that for the rigid substrate. Note that, if the test area is not defined to match the stud area, the highest stress appears at the adhesive/PDE interface. This is true for both flexible and rigid set-ups, and it is not desired as the copper/PDE interface is the target of the investigation. The stress at the adhesive/PDE interface is about 50% higher than that at the PDE/copper interface for the flexible set-up and 100% higher for the rigid set-up. Thus, the definition of the test area is mandatory to ensure that the tensile force is transmitted to the correct interface.

The stress distributions of the set-ups where the test areas are defined to match the stud area are shown in Fig. 3(c) and (d). The test pads are modelled on a flexible substrate in Fig. 3(c) and on a rigid substrate in Fig. 3(d). Both cases show that the PDE/copper interface is under the greatest stress, as desired, and it is thus more probable that the fracture starts from the PDE/copper interface than the adhesive/PDE interface. The difference in the concentrated stresses between the flexible and rigid substrates remains significant, however.

To summarise the results of the modelling, the marked stress concentration at the edges of the test area was expected to result in significantly smaller values of adhesion strength with the flexible than the rigid substrates in the experiments. Further, it was found that, with the rigid substrates, the use of a nonphotodefined test area could cause problems in the execution of adhesion test because of the possibility of fracture taking place at the adhesive/PDE interface.

3.1.2. Verification of the method—experimental results

Adhesion tests were carried out with the four PDE coating systems on copper described above, i.e. (1) the nonphotodefined and (2) the photodefined test pads on the flexible substrate and (3) the nonphotodefined and (4) the photodefined test pads on the rigid substrates. The experimental results were consistent with the findings of the FEM calculations. The PDE coating with nonphotodefined test area prepared on the rigid substrate could not be detached because the fracture took place at the adhesive/PDE interface. The FEM calculations supported this, as the stress concentration was shifted to the adhesive/PDE interface. When the test area was defined to match the stud area and the substrate was rigid, an adhesion strength value was obtained from the correct interface. In addition, the PDE/copper interface broke at lower stresses in the case of the flexible substrate (2.9 MPa) than the rigid construction (18.1 MPa). For the flexible substrate there was no significant statistical difference (T-test: $\alpha = 7.3 \times 10^{-2}$) between the adhesion results obtained for the nonphotodefined (3.3 MPa) and the defined (2.9 MPa) test areas.

Cohesive fracture within the PDE has been reported [32] to occur at adhesion strength values of about 6 MPa, which is significantly lower value than we measured with

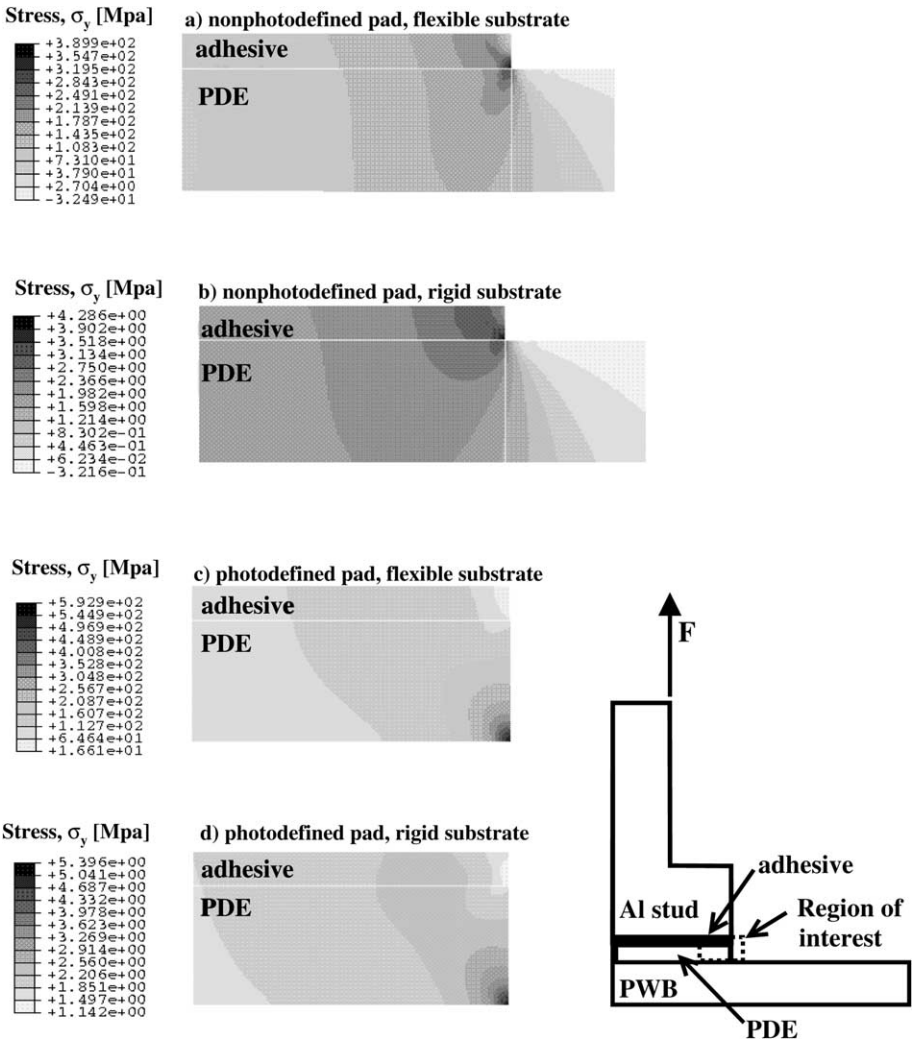

Fig. 3. Calculated tensile stress distributions in the vicinity of the stud edge: (a) the nonphotodefined test pad on flexible substrate, (b) nonphotodefined test pad on rigid substrate, (c) photodefined test pad on flexible substrate, and (d) photodefined test pad on rigid substrate.

the rigid construction. However, we did not observe cohesive but interfacial fracture. The tensile strength of the given PDE is reported to be as high as 106 ± 3 MPa [45]. One reason for the marked difference between the two adhesion strength values and the locus of fracture could be a concentration of stresses caused by bending in the first case. For a "true" bulk fracture to take place, the adhesion strength measured in the test should be of the same order of magnitude as the tensile strength of the material providing that the stress concentration and other sources of error are excluded. As stated above, the fractures in the present study took place at the interface, not in the bulk material. This is in agreement with the material properties of the PDE and supports the assumption that the adhesive forces acting between copper and the PDE are weaker than the cohesive forces of the PDE. Therefore, to obtain the "true" value of the interfacial adhesion strength, it is proposed that test samples prepared on a PWB should be attached to rigid substrates before execution of the pull-off test.

3.2. Influence of environmental exposures on adhesion

3.2.1. Characterisation of pre-treated samples

The effects of oxidation, adhesion promoter (GPS), and environmental stresses on the adhesion of the PDE to copper were examined. The usefulness of black-oxide-forming solution to promote adhesion of epoxy to copper surface is well known in the PWB industry [46]. However, the black-oxide layer consists of a mixture of

oxides, i.e. Cu_2O and CuO. To study only the effect of CuO on the adhesion, the oxidation was carried out electrolytically. Treatment time was kept to 30 s to minimise the roughening of the copper surface. Roughening should be minimal to avoid mechanical interlocking of the PDE on the surface, as this would complicate the

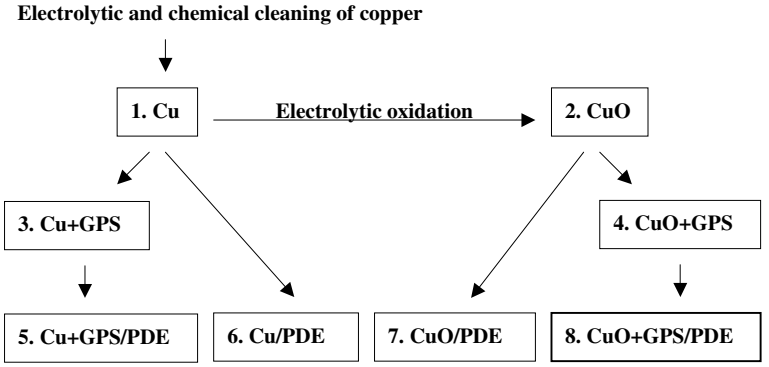

Fig. 4. Schematic presentation of the preparation of samples for XPS analysis (Samples 1–4) and adhesion characterisation (Samples 5–8).

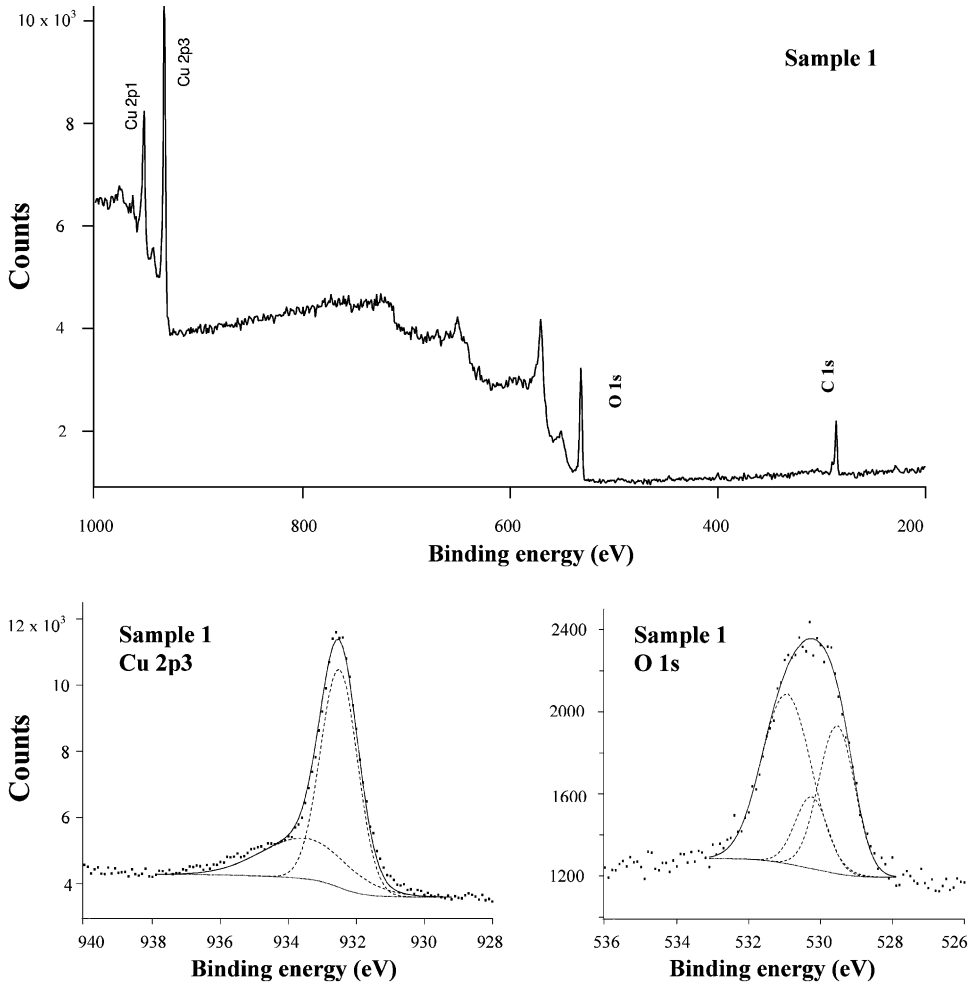

Fig. 5. Overall spectrum of Sample 1 (above), and high-resolution spectra Cu 2p3 (bottom left) and O 1s (bottom right).

interpretation of the adhesion results. Fig. 4 shows the steps in the sample preparation. The chemical state of each sample was analysed by XPS. The XPS analyses of Samples 1–4 gave information about the pre-treatments, and the adhesion tests run on Samples 5–8 revealed the effect of the treatments on adhesion.

The analysis of Sample 1 (Cu) showed that an oxidation layer is formed on the copper surface immediately after the cleaning procedure (Fig. 5). The oxygen peak at 529.6 eV corresponds to CuO, and the peak at 530.3 eV to Cu_2O. Also, a small amount of carbon-based contaminant is observed at 531.0 eV. Contamination cannot be completely avoided owing to the high surface free energy of copper and a thin adsorption layer of carbon compounds is always formed in laboratory or industrial environments. The copper peak with binding energy of 933.6 eV is assigned to CuO, and the 932.9 eV peak to both metallic copper and Cu_2O. The at.% of copper and copper oxides can be calculated from the information obtained from Cu $2p_{3/2}$ and O 1s spectra. Thus, the oxidation states of copper on the surface equal 45 at.% Cu, 25 at.% Cu_2O and 30 at.% CuO. From the XPS analysis it is impossible to know the sequence in which the species form on the surface. All the species (Cu^0, Cu^{+I} and Cu^{+II}) are simply detected to coexist within the analysable depth of the surface, which is a few nanometres. It is highly probable nevertheless that the outmost surface layer is composed of the oxidised species and the Cu^0 signal comes from beneath the oxidised layer. This would mean that the oxidised surface layer is very thin, because the Cu^0 signal is still quite strong. Exposure to normal atmosphere in laboratory or industrial conditions between the cleaning procedure and subsequent coating is sufficient for the formation of the oxide species. Therefore, the Sample 1 (Cu) surface represents the common oxidation state of the copper before coating. Although

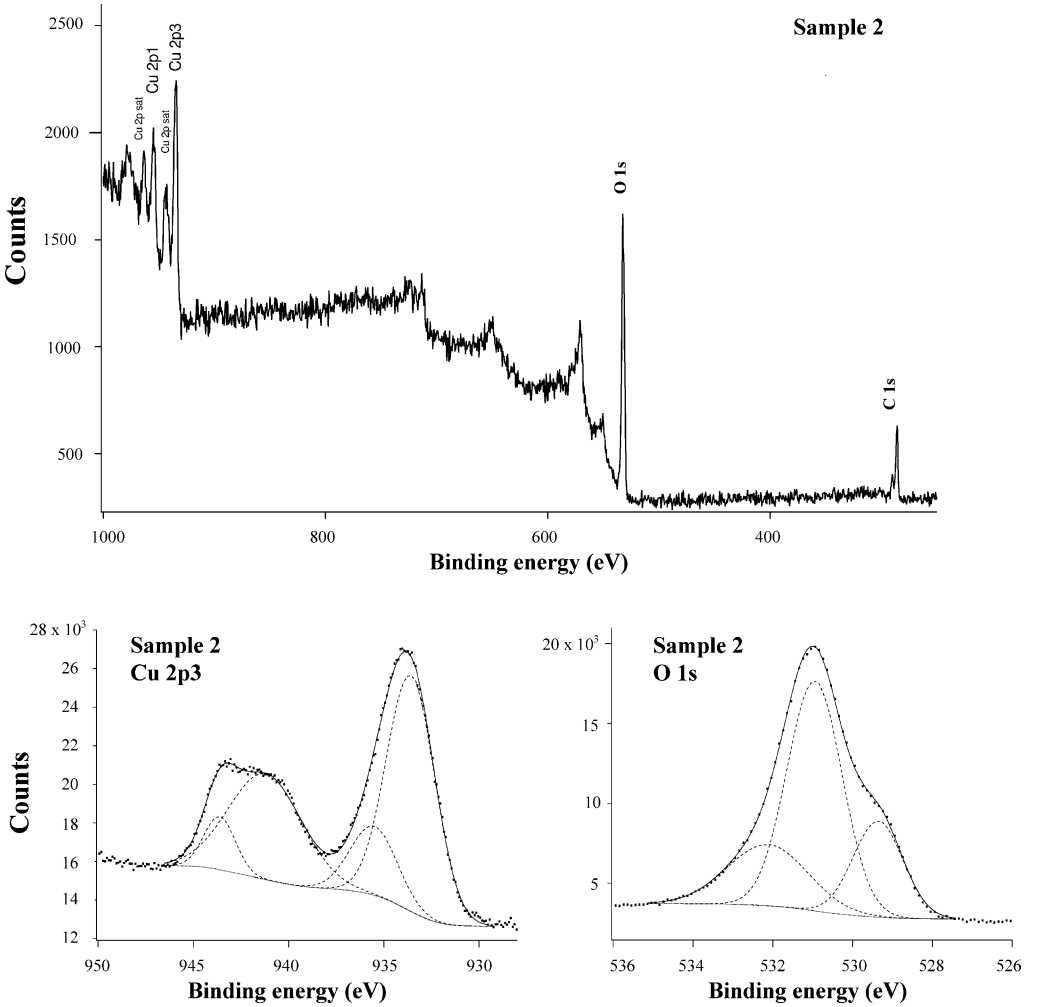

Fig. 6. Overall spectrum of Sample 2 (above), and high-resolution spectra Cu 2p3 (bottom left) and O 1s (bottom right).

the oxide growth on the copper surface is a slow process in normal atmosphere, total removal of the oxide species would require vacuum processing between the cleaning procedure and subsequent coating. Vacuum processing is not usual in PWB processing, and thus the results for the slightly oxidised copper surface better represent the real state of copper than does the totally reduced copper surface (Cu^0).

The binding energy of the copper photoelectric peak of Sample 2 (CuO) showed that the electrolytically oxidised copper surface is entirely composed of CuO (Fig. 6). This is also qualitatively verifiable from the Cu $2p_{3/2}$ spectrum, where the photoelectric peak casts a satellite peak on the high binding energy side, as reported by Moulder et al. [47]. The formation of CuO is expected on the basis of the Pourbaix diagram for copper in the aqueous solution [48].

An analysis of Samples 3 (Cu+GPS) and 4 (CuO + GPS) showed the incorporation of the GPS adhesion promoter on the copper surface. The oxygen peak fitting was adequately done with a single peak because the expected functional groups of oxygen were Si–OH, epoxy, C–O–C and CuO, which have binding energies of 532.9, 533.1, 532.6 and 529.6 eV, respectively [47,49]. The first three energies are within 0.5 eV of each other and can be explained with a single peak. Carbon peak fitting was done with 4 peaks, in accordance with the expected functionalities. The 284.3 eV peak is assumed to arise from C–Si bonds, 285.0 eV from C–C bonds, 286.2 eV from C–O–C bonds, and 287.0 eV from epoxy rings. The XPS spectra for Sample 4 are shown in Fig. 7. Table 2 presents the elemental composition of the XPS-analysed samples. The elemental composition of Samples 3 and 4 is compared to the stoichiometric

Table 2
An atomic composition (at.%, ±3 units) of the XPS-analysed Samples 1–4

	1	2	3	4
Cu	40	13	29	1
C	34	29	37	51
O	26	58	28	35
Si	–	–	6	13

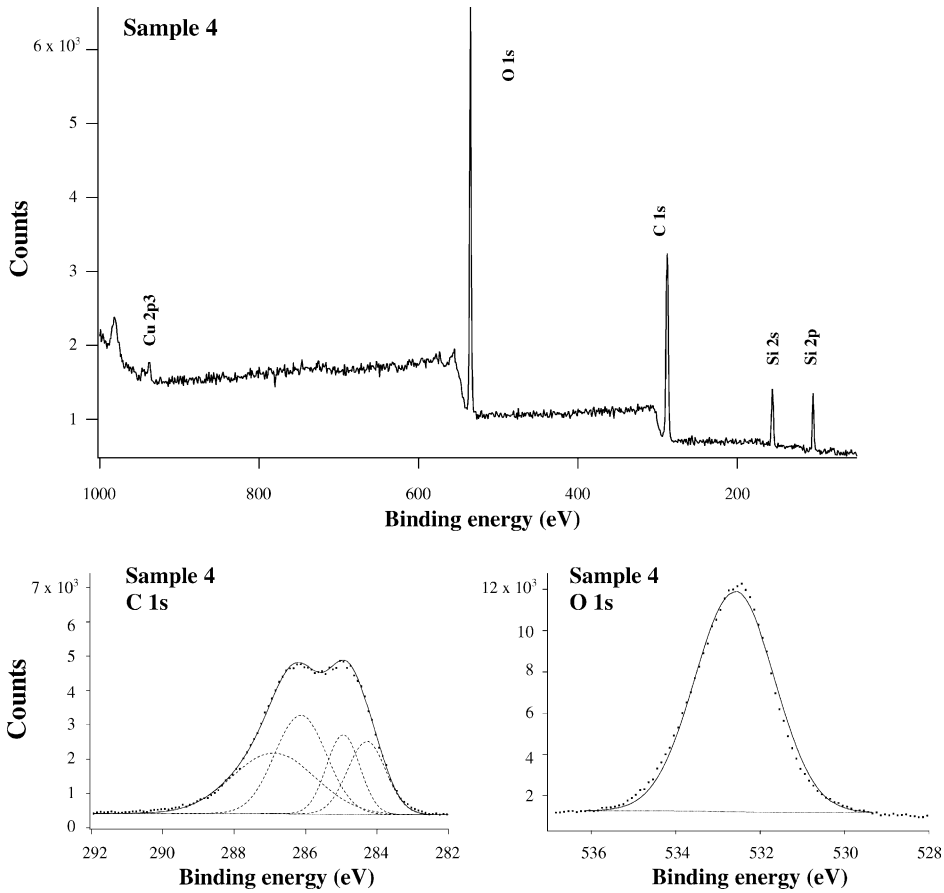

Fig. 7. Overall spectrum of Sample 4 (above), and high-resolution spectra C 1s (bottom left) and O 1s (bottom right).

composition of GPS, which is carbon (50 at.%), oxygen (42 at.%) and silicon (8 at.%). Thus, if the copper signals obtained in the analysis of the GPS-treated Samples 3 and 4 are neglected, the proportional amounts of the rest of the measured elements are 52 and 51 at.% carbon, 40 and 36 at.% oxygen, and 8 and 13 at.% silicon for Samples 3 and 4, respectively. Accordingly, the CuO surface (Sample 4) adsorbed more adhesion promoter than Sample 3.

3.2.2. Adhesion durability of the PDE and copper interface

Adhesion tests were carried out with copper clad laminated PWB, which acted as a flexible substrate. The adhesion results do not therefore represent absolute values for the adhesion but only relative values. Even the comparative results, however, reveal the deteriorating effects of the different environmental exposures. To emphasise the effects of the exposure tests, the copper surfaces were only degreased; micro-etching was not applied. Roughening of the copper surface in a micro-etch solution would have led to a mixed adhesion mechanism, i.e. incorporation of mechanical interlocking, and the interpretation of the results would have become more complicated. The adhesion of Samples 5–8 (see Fig. 4 for definition of samples) was measured immediately after their preparation as controls and after the environmental tests, and the results are shown in Fig. 8.

In the case of the Cu/PDE system (Sample 6), 85 °C/85% RH test had only a minor deteriorating effect on the adhesion, but the incorporation of corrosive gases and the temperature cycling caused noticeable degradation of the adhesion. SEM examination showed that the coatings were fractured at the copper/PDE interface, which indicates deterioration at the interface rather than loss of bulk material integrity.

The presence of an oxidation layer (CuO) (Sample 7) decreased the copper/PDE adhesion. In particular, it reduced the adhesion durability under conditions of high humidity. Lee and Kim [3] suggest that to improve adhesion in the case of CuO formation, a roughened surface should be created. The surface was not roughened here, and copper adhesion to the PDE was lost. Lee and Kim [3] also report that even a minor formation of Cu_2O would increase adhesion without any significant increase in roughness. As detected by XPS, our control copper surfaces exhibited mixed oxidation states with Cu_2O (25 at.%), CuO (30 at.%) and Cu (45 at.%). Since the control samples exhibited higher adhesion strengths and better durability than the CuO surface, we presume that the Cu_2O surface forms stronger chemical bonds with the PDE than the CuO surface.

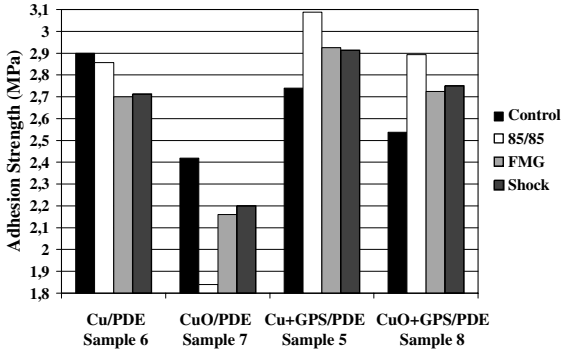

Fig. 8. An adhesion durability of treated copper/PDE systems under different environmental exposures.

The use of GPS adhesion promoter (Samples 5 and 8) did not improve the adhesion of the control sample but it effectively improved the durability of the adhesion during the environmental tests. In fact, relative to the controls the adhesion at the Cu+GPS/PDE and CuO+GPS/PDE interfaces increased during the exposures. This is proposed to result from the continuing coupling reaction of the SiOH groups of the GPS with the partially or totally oxidised copper surfaces. The GPS adhesion promoter has been shown to exhibit good water barrier properties [50,51]. Water diffusion to the interface is thus effectively blocked and the deterioration of interfacial bonds is minimised. During the shock test the materials sequentially expanded and contracted several times but in different degree, which usually causes interfacial microdelamination. However, performance in the shock test was good after the GPS treatment. The silicone-based GPS probably acts as a flexible layer between the epoxy and copper. No cracking of the coating was observed although the adhesion decreased slightly. The reliability of the interface between the PDE and oxidised copper (CuO) is enhanced as a consequence of the utilisation of the GPS.

In summary, a simple consideration of the initial adhesion strength value is not fruitful and is by no means a sufficient indication of interfacial reliability. The interfacial reliability depends on the nature of the adhering bonds, i.e. are they prone to the attack of environmental factors like moisture, etc. Actually, it was noticed that the adhesion strength was increased during the environmental exposures when the adhesion promoter was utilised. Interestingly, the results suggest that the copper surface with the mixed oxidation state including Cu_2O performed better than the CuO surface. Hence, conclusions about the interfacial reliability should not be drawn based on the initial adhesion strength, but a set of environmental exposure tests needs to be performed.

3.2.3. Capacitive monitoring—plate capacitor

Open and embedded plate capacitors were used to study the effects of environmental exposure(s) on the

dielectric material performance. The plate capacitors showed diffusion of water into the photodefinable epoxy as functions of relative humidity, temperature, and exposure time (see Fig. 9). The dielectric constant of unbound water ($\varepsilon = 75$) is significantly higher than that of PDE ($\varepsilon = 3.5$), and the absorption of water increases the dielectric constant of the PDE. Increase in capacitance thus appears as a function of the amount of absorbed water. The higher the temperature the faster was the water absorption.

The change in the capacitance of the 85 °C/85% RH exposed samples was reversible. Performance of the capacitors was gradually recovered during storage in laboratory conditions as the absorbed water was desorbed and evaporated. Interestingly, incorporation of the corrosive gases increased the capacitance more than the exposure to otherwise similar conditions but without the gases. The flowing mixed gas environment caused an irreversible weakening of the dielectric performance. It is assumed that the gaseous substances form ions in the presence of water, which are then bound in the photodefinable epoxy and increase the dielectric constant. SO_2, for example, has been reported to form bisulphate ions (HSO_4^-) [52]. The electrical characterisation showed resistance between the plates, but no capacitance could be measured for most of the capacitors after the 1000-h exposure. This means that the photodefinable epoxy eventually began to behave more as a high resistance conductor than as a dielectric material. The capacitors were considered as failed once they showed more than 50% change in capacitance relative to the initial value. The uncoated plate capacitors began to fail after seven days exposure to the FMG conditions (2% of the capacitors), while the coated capacitors showed only increased capacitance. Nevertheless, after 14 days in FMG conditions, the coated plate capacitors failed almost totally (92%), while the failure rate of the uncoated samples was only 67%. The capacitive monitoring in the FMG chamber was halted after 14 days owing to the high failure rate. It is not yet clear why the coated plate capacitors performed worse than the uncoated ones.

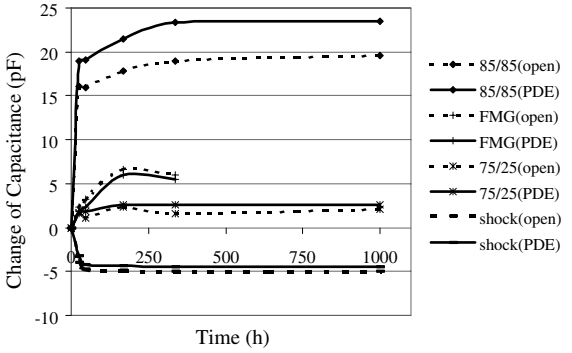

Fig. 9. Change of capacitance (pF) in open and PDE coated plate capacitors as a function of the exposure time to 85% RH/85 °C, flowing mixed gas, 75% RH/25 °C, and thermal shock conditions.

The mismatch in the coefficients of thermal expansion of copper (16.8 ppm) and the PDE (50 ppm) caused some micro-delamination during the thermal cycling. This was detected as a slight decrease in the capacitance of the shock-tested plate capacitors (Fig. 9). It is expected that air ($\varepsilon = 1$) fills the cavities created by the early delamination and thereby reduces the capacitance.

3.2.4. Capacitive monitoring—interdigital capacitor

Electrochemical migration of copper was observed with an open interdigital capacitor that was exposed either to 85 °C/85% RH or to FMG test in the biased

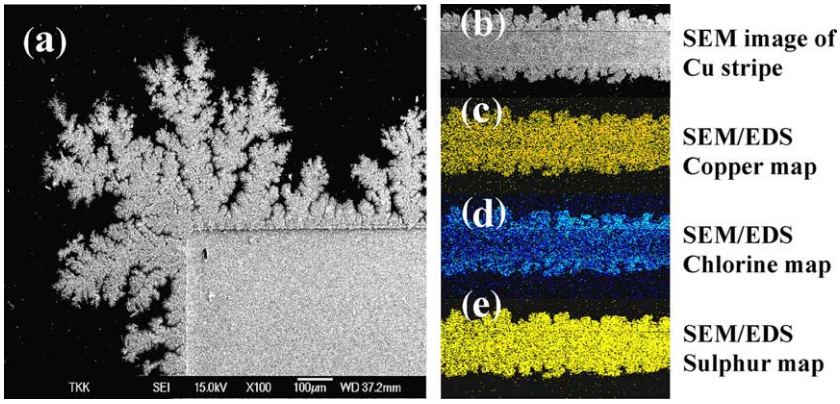

Fig. 10. SEM micrograph (a) of a comer of an open interdigital capacitor after exposure to flowing mixed gas test in electrically biased mode. Significant electrochemical migration of the corrosion products can be seen in SEM image of the anode-connected copper finger of the capacitor (b) SEM/EDS elemental mapping of the finger shows that the corrosion products contain (c) copper, (d) chlorine and (e) sulphur.

(9.0 V) mode (Fig. 10(a)). Closer examination of an anode-connected finger (Fig. 10(b)) with SEM/EDS elemental mapping (Fig. 10(c)–(e)) showed that, in the FMG test, the gases caused the corrosion of copper, with the formation of sulphur and chlorine compounds, which began to migrate in the electric field. The embedded capacitors, in contrast, exhibited only increased capacitance during the 85 °C/85% RH and FMG tests, and electrochemically produced shorts were not observed.

4. Conclusions

The widely used pull-off adhesion test was evaluated for use in the assessment of epoxy adhesion to printed wiring board (PWB) metallisation. Finite element method (FEM) calculations were used to identify the weaknesses of the pull-off method and to help in the design of a more reliable adhesion test. Modelling showed that the use of flexible substrate results in lower values of adhesion strength than when rigid substrate is used because the tensile stresses are highly concentrated near the edges of the stud in the flexible construction. A copper clad laminated PWB substrate that is 1 mm in thickness acts as a flexible substrate in the pull-off test. It was also revealed that, with a flexible substrate, the stress appears at the adhesive/PDE interface rather than at the region of interest, i.e. the PDE/copper interface, if the area to be tested was not defined to match the area of the stud of the test equipment. It is proposed that the most reliable results are obtained with a construction that is prepared on a rigid substrate and uses defined test areas. The experimental data were in agreement with the results of the FEM calculations.

Adhesion durability of the Cu/PDE interface was investigated in several environmental stress tests. The stresses were induced by the controlled exposure of the samples to (1) temperature cycling, (2) elevated temperature and relative humidity and (3) the environmental pollutants. The adhesion between the oxidised copper surface (CuO) and the PDE was noticeably reduced during the tests, whereas the properly purified copper performed relatively reliably. Utilisation of adhesion promoter 3-glysidoxy propyl trimethoxy silane (GPS) enhanced the adhesion of the oxidised Cu and, in particular, improved the durability of the adhesion in the environmental tests. The GPS served as a flexible interlayer in the thermal shock test and samples containing GPS performed well in the test. However, GPS did not significantly improve the reliability when it was used with the purified copper. The capacitive monitoring showed that the PDE coating protects the structure from electrochemical migration but is a poor diffusion barrier against water. In addition, the corrosive gases were absorbed into the PDE and the dielectric performance of the PDE was lost, irreversibly. In the present study, better understanding was gained of the pull-off adhesion test method and of the environmental factors affecting the adhesion at the copper/PDE interface. The findings will assist in the fabrication of more reliable consumer electronics.

Acknowledgements

The authors would like to thank Dr. Kari Lounatmaa for his contribution to the SEM study, Dr. Tomi Laurila for his useful comments, and Mr. Andrei Olykainen for technical assistance in the adhesion testing. The Finnish Center for Scientific Computing provided the computing facilities and the Academy of Finland provided financial support.

References

[1] Martin PL, editor. Electronic failure analysis handbook. New York: McGraw Hill; 1999.
[2] Kujala A, Tuominen R, Kivilahti JK. Solderless interconnection and packaging technique for embedded active components. In: Proceedings of 49th Electronic Component Technology Conference. San Diego, CA, USA, June 1–4, 1999. p. 155–9.
[3] Lee HY, Kim SR. Pull-out behavior of oxidized copper leadframes from epoxy molding compounds. J Adhes Sci Technol 2002;16:621–51.
[4] Mittal KL, editor. Adhesion measurement of films and coatings. Utrecht, The Netherlands: VPS; 1995.
[5] Kinloch AJ, editor. Durability of structural adhesives. London: Elsevier Applied Science; 1983.
[6] Stepniak F. Failure criteria of flip chip joints during accelerated testing. Microelectron Reliab 2002;42:1921–30.
[7] Puligandla V, Singh P. Failure modes and mechanisms in electronic packages. New York: Chapman and Hall; 1998.
[8] Francis LF, McCormick AV, Vaessen DM, Payne JA. Development and measurement of stress in polymer coatings. J Mater Sci 2002;37:4717–31.
[9] Sato K. The internal stress of coating films. Prog Org Coat 1980;8:143–60.
[10] Thouless MD. Decohesion of films with axisymmetric geometries. Acta Metall 1988;36:3131–5.
[11] Jacques LFE. Accelerated and outdoor/natural exposure testing of coatings. Prog Polym Sci 2000;25:1337–62.
[12] Negele O, Funke W. Internal stress and wet adhesion of organic coatings. Prog Org Coat 1996;28:285–9.
[13] Bower DI. An introduction to polymer physics. Cambridge: Cambridge University Press; 2002.
[14] Lawrence S, Willett JL, Carriere CJ. Effect of moisture on the tensile properties of poly(hydroxy ester ether). Polymer 2001;42:5643–50.
[15] Loh WK, Crocombe AD, Abdel Wahab MM, Watts JF, Ashcroft IA. The effect of moisture on the failure locus and

fracture energy of an epoxy—steel interface. J Adhes Sci Technol 2002;16(11):1407–29.
[16] Bellenger V, Ganem M, Mortaigne B, Verdu J. Lifetime prediction in the hydrolytic ageing of polyesters. Polym Degrad Stab 1995;49:91–7.
[17] Liu J, Lai Z, Kristiansen H, Khoo C. Overview of conductive adhesive joining technology in electronics packaging applications. In: Proceedings of the 3rd International Conference on Adhesive Joining and Coating Technology in Electronics Manufacturing. Binghamton, NY, USA, September 28–30, 1998. p. 1–18.
[18] Kinloch AJ, Little MSG, Watts JF. The role of the interphase in the environmental failure of adhesive joints. Acta Mater 2000;48:4543–53.
[19] Hamade RF, Dillard DA. Cathodic weakening of elastomer-to-metal adhesive bonds: accelerated testing and modelling. J Adhes Sci Technol 2003;17(9):1235–64.
[20] Leidheiser Jr H, Wang W, Igetoft L. The mechanism for the cathodic delamination of organic coatings from a metal surface. Prog Org Coat 1983;11(1):19–40.
[21] Banks WM, Dumolin F, Halliday ST, Hayward D, Li Z-C, Pethrick RA. Dielectric and mechanical assessment of water ingress into carbon fibre composite materials. Comput Struct 2000;76:43–55.
[22] Lim K-B, Lee B-S, Lee D-C. A study on the surface change and dielectric properties of epoxy insulator by water degradation. In: Proceedings of 1998 International Symposium on Electrical Insulating Materials. Toyohashi, Japan, September 27–30, 1998. p. 293–6.
[23] Harsányi G. Electrochemical processes resulting in migrated short failures in microelectronics. IEEE Trans Compon Pack Manuf Technol Part A 1995;16(3):207–16.
[24] Gore RR, Witska R, Kirby JR, Chao JL. Corrosive gas environmental testing for electrical contacts. IEEE Trans Compon Hybr Manuf Technol 1990;13(1):27–32.
[25] Abbott WH. The development and performance characteristics of mixed flowing gas test environment. IEEE Trans Compon Hybr Manuf Technol 1988;11(1):22–35.
[26] International standard for environmental testing. Part 2: Tests: Flowing mixed gas corrosion test. IEC 68-2-60, 1995.
[27] Geckle RJ, Mroczkowski RS. Corrosion of precious metal plated copper alloys due to mixed flowing gas exposure. IEEE Trans Compon Hybr Manuf Technol 1991;14(1):162–9.
[28] Svedung OA, Johansson L-G, Vannerberg N-G. The influence of NO_2 and Cl_2 at low concentrations in humid atmospheres on the corrosion of gold-coated contact materials. IEEE Trans Compon Hybr Manuf Technol 1986;9(3):286–92.
[29] Abbott WH, Neer JH, Healey HJ. Effects of test procedures and sequences on the performance of tin-plated connectors. In: Proceedings of the Thirty-ninth IEEE Holm Conference on Electrical Contacts. September 27–29, 1993. p. 191–204.
[30] Abbott WH. The corrosion of copper and porous gold in flowing mixed gas environments. IEEE Trans Compon Hybr Manuf Technol 1990;13(1):40–5.
[31] Hillman C, Castillo B, Pecht M. Diffusion and absorption of corrosive gases in electronic encapsulants. Microelectron Reliab 2003;43:635–43.
[32] Ge J, Kivilahti JK. Effects of surface treatments on the adhesion of Cu and Cr/Cu metallizations to a multifunctional photoresist. J Appl Phys 2002;92(6):3007–15.
[33] Ge J, Turunen MPK, Kivilahti JK. Surface modification and characterization of photodefinable epoxy/copper systems. Thin Solid Films 2003;440(1–2):198–207.
[34] Ge J, Tuominen R, Kivilahti JK. Adhesion of electrolessly-deposited copper to photosensitive epoxy. J Adhes Sci Technol 2001;15:1133–43.
[35] Ge J, Turunen MPK, Kivilahti JK. Surface modification of a liquid-crystalline polymer for copper metallization. J Polym Sci, Part B: Polym Phys 2003;41:623–36.
[36] Ge J, Turunen MPK, Kivilahti JK. Effects of surface treatment on the adhesion of copper to a hybrid polymer material. J Mater Res 2003;18(11):2697–707.
[37] Marsh J, Minel L, Barthés-Labrousse MG, Gorse D. Interaction of epoxy model molecules with aluminium, anodized titanium and copper surfaces: an XPS study. Appl Surf Sci 1998;133:270–86.
[38] Brewis DM, Briggs D, editors. Industrial adhesion problems. Oxford: Orbital Press; 1985.
[39] Kinloch AJ. Adhesion and adhesives: science and technology. London: Chapman and Hall; 1987.
[40] Kinloch AJ. The science of adhesion. Part 2: Mechanics and mechanisms of failure. J Mater Sci 1982;17:617–51.
[41] Abdelkader AF, White JR. Influence of relative humidity on the development of internal stresses in epoxy resin based coatings. J Mater Sci 2002;37:4769–73.
[42] Jachim JA, Freeman GB, Turbini LJ. Use of surface insulation resistance and contact angle measurements to characterize the interactions of three water soluble fluxes with FR-4 substrates. IEEE Trans Compon Pack Manuf Technol Part B 1997;20(4):443–51.
[43] Turunen MPK, Laurila T, Kivilahti JK. Evaluation of the surface free energy of spin-coated photodefinable epoxy. J Polym Sci, Part B: Polym Phys 2002;40:2137–49.
[44] Shirley DA. High-resolution X-ray photoemission spectrum of the valence bands of gold. Phys Rev B 1972;5(12):4709–14.
[45] Feng R, Farris RJ. The characterization of thermal and elastic constants for an epoxy photoresist SU8 coating. J Mater Sci 2002;37:4793–9.
[46] Yun HK, Cho K, An JH, Park CE. Adhesion improvement of copper epoxy joints. J Mater Sci 1992;27:5811–7.
[47] Moulder JF, Stickle WF, Sobol PE, Bomden KD. Handbook of X-ray photoelectron spectroscopy: a reference book of standard spectra for identification and interpretation of XPS data. London: Physical Electronics; 1995.
[48] Pourbaix M. Atlas of electrochemical equilibria in aqueous solutions. Houston: NACE; 1974.
[49] Beamson G, Briggs D. High resolution XPS of organic polymers. London, England: John Wiley & Sons; 1992.
[50] Welsh DJ, Pearson RA, Luo S, Wong CP. Fundamental study on adhesion improvement for underfill using adhesion promoter. In: Proceedings of the 51st IEEE Electronic Components and Technology Conference. Orlando, FL, USA, May 21–June 1, 2001. p. 1502–6.

[51] Iannuzzi M. Bias humidity performance and failure mechanisms of nonhermetic aluminium SIC's in an environment contaminated with Cl_2. IEEE Trans Compon Hybr Manuf Technol 1983;6(2):191–201.

[52] Payer JH, Ball G, Rickett BI, Kim HS. Role of transport properties in corrosion product growth. Mater Sci Eng A 1995;198:91–102.